Showcasing research from the group of Dr Jongho Jeon at RI-Biomics center, Korea Atomic Energy Research Institute, Republic of Korea.

Efficient and stable radiolabeling of polycyclic aromatic hydrocarbon assemblies: *in vivo* imaging of diesel exhaust particulates in mice

To investigate *in vivo* behaviors of polycyclic aromatic hydrocarbons from diesel exhaust, radiolabeled carbonaceous particulates were synthesized in an efficient manner. SPECT images revealed high uptake and slow clearance of this matter in the respiratory system, which may underlie its severe toxicity.

As featured in:

See Jongho Jeon *et al.*, *Chem. Commun.*, 2019, **55**, 447.

ROYAL SOCIETY OF CHEMISTRY | Celebrating IYPT 2019

rsc.li/chemcomm

Registered charity number: 207890

ChemComm

COMMUNICATION

View Article Online
View Journal | View Issue

Cite this: *Chem. Commun.*, 2019, 55, 447

Received 17th October 2018,
Accepted 13th November 2018

DOI: 10.1039/c8cc08304e

rsc.li/chemcomm

Efficient and stable radiolabeling of polycyclic aromatic hydrocarbon assemblies: *in vivo* imaging of diesel exhaust particulates in mice†

Chang Heon Lee,‡[a] Ha Eun Shim,‡[a] Lee Song,[a] Hi Gyu Moon,[b] Kyuhong Lee,[b] Jung Eun Yang,[c] Ha Yeon Song,[a] Yong Jun Choi,[d] Dae Seong Choi[a] and Jongho Jeon *[ae]

As a robust radioanalytical method for tracking carbonaceous particulates *in vivo*, polycyclic aromatic hydrocarbons from diesel exhaust were labeled with a radioactive-iodine-tagged pyrene analogue. Single-photon emission computed tomography and biodistribution studies showed high uptake and slow clearance of this matter in the respiratory system, which may underlie its severe toxicity.

Diesel exhaust particulates (DEP) from diesel-fueled engines are of severe concern because of their profound adverse effects on human health and the environment.[1–3] Recently, the International Agency for Research on Cancer (IARC) has classified diesel emissions as a group 1 (carcinogenic with sufficient evidence) human carcinogen.[4] In addition, several toxicological studies have reported that exposure to diesel exhaust results in respiratory diseases such as chronic obstructive pulmonary disease (COPD), asthma, and lung cancer.[5–7] Furthermore, DEP deposited in the lungs can be distributed throughout the entire body, resulting in systemic inflammation, oxidative stress, and genotoxicity. Therefore, the inhalation of diesel exhaust may also have various toxic effects on the extrapulmonary organs, including vascular dysfunction.[1,8] DEP is a complex mixture, in which the solid fraction mainly consists of various organic substances, including polycyclic aromatic hydrocarbons (PAHs). As there are various toxicological concerns associated with PAHs, these substances have also been classified as priority pollutants.[9,10] The size of particulate matter has been identified as the main cause of the associated health problems.[11] In general, smaller particles can penetrate more deeply, allowing uptake by the respiratory organs at higher rates. The size of DEP has been observed to be in the submicrometer range; thus, the majority of DEP is small enough to accumulate in the deep lung tissue.[12]

To better understand the human health risks associated with the exposure to toxic substances, it is essential to characterize the interactions and behavior of such substances in living subjects. Many studies have reported the adverse effects of DEP in the pulmonary organs and other internal organs of both animals and humans. By contrast, quantitative assessment of the biological uptake is difficult owing to issues associated with detection in biological samples. Indeed, mass spectrometry, which is an analytical method usually used for detecting molecules, is unsuitable to analyze DEP in tissues, as DEP comprises agglomerates of various PAHs with a wide particle size distribution. Optical imaging techniques using fluorescent tags have frequently been applied to trace molecules *in vivo*. However, accurate quantification of molecules in deep tissues is often hampered by low penetration depth of optical signals. These limitations can be overcome by using a radionuclide as a tracer, which allows straightforward, accurate, and sensitive detection *in vivo*. Previously, the incorporation of radioisotopes with long-half-lives such as carbon-14 and cesium-134 into DEP has been used to assess the biological uptake in animals.[13] These studies mainly focused on the clearance kinetics of DEP from the body, whereas limited information was provided about the biological distribution in the internal organs. Non-invasive imaging has potential as an alternative useful technique for investigating the *in vivo* uptake of hazardous materials. However, because the radioisotopes used in previous studies cannot be utilized with nuclear imaging instruments, *in vivo* imaging results have not been reported. In this study, we applied a convenient and efficient radioisotope-labeling method to conduct a bioimaging study and quantify the biological uptake and accumulation of DEP in tissues.

Fig. 1 illustrates the study design, which incorporates biodistribution studies and whole-body single-photon emission computed tomography (SPECT) imaging based on radiolabeled

[a] *Advanced Radiation Technology Institute, Korea Atomic Energy Research Institute, Jeongeup 56212, Republic of Korea. E-mail: jeonj@kaeri.re.kr*
[b] *Jeonbuk Department of Inhalation Research, Korea Institute of Toxicology, Jeongeup 56212, Republic of Korea*
[c] *World Institute of Kimchi, Gwangju 61755, Republic of Korea*
[d] *School of Environmental Engineering, University of Seoul, Seoul 02504, Republic of Korea*
[e] *Radiation Biotechnology and Applied Radioisotope Science, University of Science and Technology, Daejeon 34113, Republic of Korea*

† Electronic supplementary information (ESI) available. See DOI: 10.1039/c8cc08304e

‡ These authors contributed equally to this work.

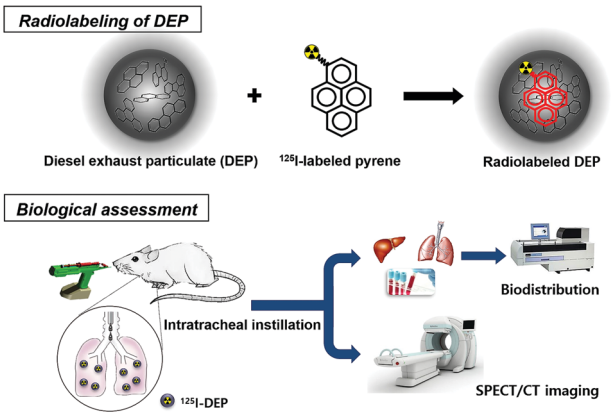

Fig. 1 The main strategy for single-photon emission computed tomography (SPECT) imaging and biodistribution studies using radioactive-iodine-incorporated diesel exhaust particulates (DEP).

DEP. First, radioactive-iodine-incorporated DEP (^{125}I-DEP) was prepared using a standard reference material, namely, DEP (SRM®2975), and an ^{125}I-labeled pyrene analogue. The self-assembled ^{125}I-DEP suspended in water was then administered to mice to visualize the *in vivo* behavior of DEP.

To prepare the radioactive-iodine-labeled pyrene, stannylated precursor **2** was synthesized as shown in Fig. S1 (ESI†). Electrophilic substitution of **2** was achieved using [^{125}I]NaI in the presence of chloramine-T as an oxidant at room temperature to give the desired product, [^{125}I]**1** (Fig. 2a). After purification of the crude mixture by preparative HPLC, [^{125}I]**1** was obtained with a radiochemical yield of 32% ± 4% (n = 3). Analytical HPLC

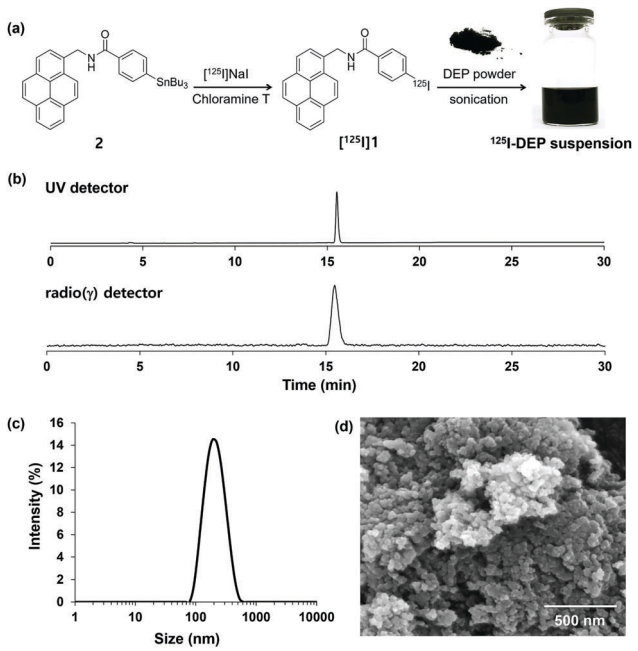

Fig. 2 Preparation and characterization of radiolabeled DEP. (a) Scheme for the synthesis of ^{125}I-DEP using the ^{125}I-labeled pyrene analogue. (b) Analytical HPLC chromatograms of purified [^{125}I]**1**. (c) Size distribution of DEP agglomerates. (d) SEM image of the DEP suspension.

revealed that [^{125}I]**1** had a radiochemical purity of more than 99% and a retention time corresponding to that of the nonradioactive reference material **1** (Fig. 2b). For further experiments, the purified product was trapped in a C-18 light cartridge, eluted using absolute ethanol, and then dried under high vacuum.

To prepare a radiolabeled DEP suspension in water, the standard DEP reference material and [^{125}I]**1** were dissolved separately in dichloromethane (DCM). These solutions were mixed together at room temperature and then DCM was removed by blowing nitrogen gas at room temperature. Distilled water was added to the dried hydrocarbon mixture, which was then ultrasonicated at an elevated temperature to obtain the radioactive-iodine-incorporated DEP suspension in water. The product (^{125}I-DEP) was subjected to centrifugal filtration (MW = 5k) to verify the assembly of [^{125}I]**1** with DEP. As most of the radioactivity was detected in the hydrocarbon pellets (less than 1% in the supernatant, as determined using a radioactive detector), radioactive iodine was successfully incorporated into the hydrocarbon matter. As shown in Fig. 2c, the hydrodynamic size distribution of the DEP suspension mostly falls between 80 and 700 nm, with an average size of approximately 190 nm. Because the amount of ^{125}I-labeled pyrene (approximately 30 ng) used in the radiolabeling step was much smaller than that of DEP (1.5 mg), the addition of the radiolabeled pyrene group ([^{125}I]**1**) should have very little effect on the physical properties of the DEP suspension, such as the size and surface charge of the particulates. Scanning electron microscopy (SEM) images of the DEP revealed that the primary particle size was less than 100 nm, and larger agglomerates were also observed in aqueous media (Fig. 2d and Fig. S2, ESI†). To determine the *in vitro* stability, the radiolabeled DEP suspension was mixed with mouse serum. As shown in Fig. S3 (ESI†), approximately 93% of ^{125}I was retained in the DEP for up to 7 days of immersion in mouse serum. Taken together, the preparation of stable radiolabeled DEP was successfully established. Therefore, it was applied in subsequent biological experiments.

As the lung is the primary organ invaded by DEP, we first administrated the radiolabeled DEP *via* intratracheal instillation. In a typical animal experiment, approximately 3.7 MBq of radioactivity was administered per mouse. Whole-body SPECT images clearly revealed that ^{125}I-DEP was primarily accumulated in the lungs after intratracheal instillation (Fig. 3a). Moreover, a strong signal was still observed in the respiratory system after 48 h, whereas most of the signals in the other organs, including the intestines, diminished significantly. The amounts of radioactivity accumulated in the blood and tissues are plotted in Fig. 3b as a percentage of the injected dose (% ID). Notably, high levels of ^{125}I-DEP were detected in the lungs 0.5 h post administration, which then slowly decreased, with approximately 61% of the initial uptake value retained after 48 h. In addition, DEP was also observed in the liver and intestines, suggesting that some DEP underwent hepatobiliary clearance. Some ^{125}I-DEP may have been swallowed into the stomach during instillation, as uptake was also detected in the digestive organs. To examine the absorption and translocation through the intestines to other internal organs, we administered the ^{125}I-DEP suspension *via*

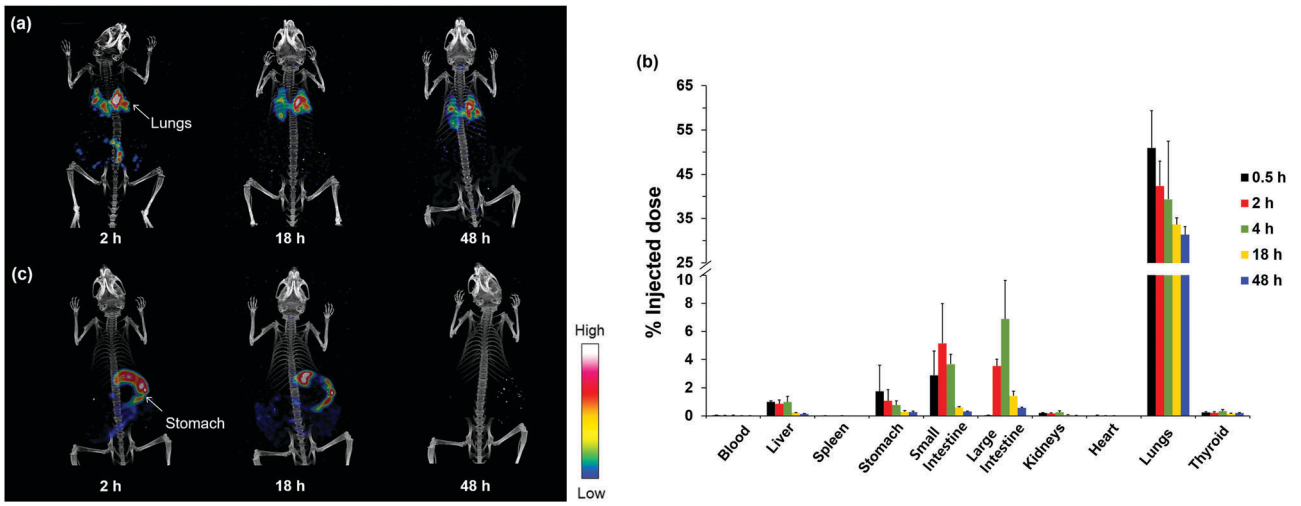

Fig. 3 (a) Whole-body SPECT/CT images over 48 h of intratracheally instilled ^{125}I-DEP in an ICR mouse. (b) Biological distribution of intratracheally instilled ^{125}I-DEP in nine different organs and the blood (n = 4). Data is expressed as a percent of the injected dose (% ID). (Data in Fig. S4, ESI† is expressed as % ID/gram tissue.) (c) Whole-body SPECT/CT images over 48 h of orally administered ^{125}I-DEP in an ICR mouse.

oral gavage. As shown in Fig. 3c, orally administered DEP had little effect on lung accumulation, and ^{125}I-DEP was excreted within 2 days, with no significant uptake in the extraintestinal organs such as the lungs, liver, and spleen. These results indicate that the accumulation of ^{125}I-DEP in the lungs mainly results from uptake into the respiratory system, not from translocation from the gastrointestinal tract. These observations highlight the value of investigating DEP accumulation *via* different administration routes to analyze the *in vivo* behavior of DEP.

To investigate how nanosized DEP agglomerates comprising PAHs affect the level of translocation to other organs, we conducted a comparison experiment with ^{125}I-pyrene ([^{125}I]**1**), a small molecule, which was administered to mice *via* intratracheal instillation. Remarkably, different uptake and clearance patterns were observed, as shown by the SPECT images (Fig. 4a and Fig. S5, ESI†). Strikingly, ^{125}I-pyrene, which does not form nanoscale structures, accumulated in the lungs at much lower levels than ^{125}I-DEP, and was mostly cleared within 48 h (Fig. 4b). Bright signals were observed in the gallbladder and intestines, suggesting that most of the radiolabeled pyrene underwent rapid hepatobiliary excretion. By contrast, for instilled agglomerates comprising DEP molecules, with average sizes of several hundred nanometers, as only part of these materials might be transported to other organs, they were cleared slowly (Fig. 3a and b). These results were in accordance with several previous studies reporting that larger particles pass through the air–blood barrier in the respiratory system more slowly than smaller molecules and are thus accumulated more heavily in the lungs.[14–16]

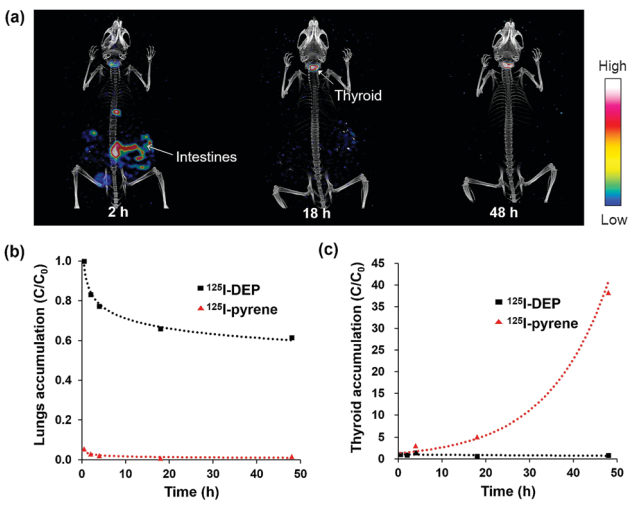

Fig. 4 (a) Whole-body SPECT/CT images over 48 h of intratracheally instilled ^{125}I-pyrene ([^{125}I]**1**) in an ICR mouse. (b and c) Accumulation of intratracheally instilled ^{125}I-DEP and ^{125}I-pyrene in the lungs and thyroid, respectively. C_0 indicates the amount of ^{125}I-DEP in the organs 0.5 h post administration.

The thyroid uptake values reflect the *in vivo* stability of the radioactive-iodine-labeled product because the released free iodine ions (I^-) rapidly accumulate in the thyroid.[17,18] A comparison of both the thyroid uptake values (Fig. 4c) and the SPECT/CT images revealed that only a small amount of $^{125}I^-$ (as low as 0.5% ID) from the radiolabeled DEP was detected 48 h post administration (Fig. 3a). Therefore, ^{125}I-DEP retained its stability *in vivo*, which allowed a reliable determination of the ^{125}I-DEP biodistribution, with little release of $^{125}I^-$ from DEP.

Notably, the biological impact of various hazardous materials has been investigated using radioisotopes.[19–25] A few radiolabeled products have been useful for noninvasive imaging and quantification of the biological uptake of small molecules or macromolecules. In the case of DEP agglomerates with a wide range of sizes, it is difficult to apply a direct radiolabeling method because DEP does not contain a suitable functional group for radioisotope tagging. In our protocol, the use of radiolabeled pyrene ([^{125}I]**1**) allowed a simple and efficient preparation of a radioisotope-incorporated DEP suspension. Owing to its aromaticity and hydrophobicity, [^{125}I]**1** easily interacts with DEP through π–π stacking, forming stable hybrids in aqueous media. Indeed, [^{125}I]**1** assembled with DEP exhibited high stability both in

serum (Fig. S3, ESI†) and in mice, which enabled accurate *in vivo* tracing of ^{125}I-DEP.

In this work, we primarily focused on the development of a radiolabeling method and an initial *in vivo* evaluation using radiolabeled particulates. Our results suggest that further long-term observations are necessary to determine the size-dependent *in vivo* distribution, translocation, and excretion kinetics of DEP. It has been reported that many other kinds of particulate matters also consist of PAHs. Therefore, the radioanalytical method developed in this study can also be applied to *in vivo* assessments of these hazardous materials. In addition, noncovalent interactions between aromatic carbons have been used to functionalize graphene and graphene oxide for biomedical applications, such as biosensors, bioimaging, and disease therapy.[26,27] Because a lot of pyrene derivatives showed high toxicity in cells, the cytotoxicity of **1** was assessed using three different cell lines. The assay results revealed that the iodine-labeled pyrene did not exhibit significant cytotoxicity up to 0.5 μM, the administered concentration of the compound for the animal imaging study (Fig. S6, ESI†). These observations suggested that radioactive-iodine-labeled pyrene ([^{125}I]**1**) can become the method of choice for the simple preparation of useful *in vivo* radiotracers.

In conclusion, we have described an efficient radiolabeling and radioanalytical method for conducting non-invasive *in vivo* imaging of DEP, a hazardous fine particulate, and biodistribution studies in mice *via* intratracheal instillation. The molecular imaging and biodistribution data clearly demonstrated that high levels of DEP accumulate in the lungs, and this mechanism may underlie the observed fatal toxic effects. These results provide important information on the behavior of harmful chemicals in living subjects, which may ultimately prove valuable in modeling the health effects in a large population and in environmental epidemiology. Moreover, our method is not limited to DEP but can be extended to the assessment of other polyaromatic-hydrocarbon-based environmentally toxic particulates and synthetic materials.

This study was funded by the National Research Foundation of Korea (Grant number: 2017M2A2A6A01070858).

Conflicts of interest

There are no conflicts to declare.

Notes and references

1 S. Steiner, C. Bisig, A. Petri-Fink and B. Rothen-Rutishauser, *Arch. Toxicol.*, 2016, **90**, 1541–1553.
2 D. Wu, F. Zhang, W. Lou, D. Li and J. Chen, *Sci. Total Environ*, 2017, **605–606**, 172–179.
3 H. Shen, S. Tao, J. Liu, Y. Huang, H. Chen, W. Li, Y. Zhang, Y. Chen, S. Su, N. Lin, Y. Xu, B. Li, X. Wang and W. Liu, *Sci. Rep.*, 2014, **4**, 6561.
4 X. Zheng, Y. Wu, S. Zhang, J. Hu, K. M. Zhang, Z. Li, L. He and J. Hao, *Sci. Rep.*, 2017, **7**, 10058.
5 I. A. Yang, V. Relan, C. M. Wright, M. R. Davidson, K. B. Sriram, S. M. Savarimuthu Francis, B. E. Clarke, E. E. Duhig, R. V. Bowman and K. M. Fong, *Expert Opin. Ther. Targets*, 2011, **15**, 439–456.
6 D. T. Silverman, C. M. Samanic, J. H. Lubin, A. E. Blair, P. A. Stewart, R. Vermeulen, J. B. Coble, N. Rothman, P. L. Schleiff, W. D. Travis, R. G. Ziegler, S. Wacholder and M. D. Attfield, *J. Natl. Cancer Inst.*, 2012, **104**, 855–868.
7 N. E. Alexis and C. Carlsten, *Int. Immunopharmacol.*, 2014, **23**, 347–355.
8 M. Miller, S. G. McLean, C. A. Shaw, R. Duffin, A. O. Lawal, J. A. Araujo, P. W. F. Hadoke and D. E. Newby, *Atherosclerosis*, 2015, **241**, e137–e138.
9 M. Shrivastava, S. Lou, A. Zelenyuk, R. C. Easter, R. A. Corley, B. D. Thrall, P. J. Rasch, J. D. Fast, S. L. Massey Simonich, H. Shen and S. Tao, *Proc. Natl. Acad. Sci. U. S. A.*, 2017, **114**, 1246–1251.
10 M. M. Pratt, P. Sirajuddin, P. E. Castle, D. H. Phillips, S. Afework, A. B. Maclean, N. Ragavan, F. L. Martin, R. J. Šrám, D. K. Manchester, O. A. Olivero and M. C. Poirier, *Proc. Amer. Assoc. Cancer Res.*, 2006, **47**, 486.
11 K.-H. Kim, E. Kabir and S. Kabir, *Environ. Int.*, 2015, **74**, 136–143.
12 M. R. Miller, S. G. McLean, R. Duffin, A. O. Lawal, J. A. Araujo, C. A. Shaw, N. L. Mills, K. Donaldson, D. E. Newby and P. W. F. Hadoke, *Part. Fibre Toxicol.*, 2013, **10**, 61.
13 T. W. Hesterberg, W. B. Bunn, R. O. McClellan, G. A. Hart and C. A. Lapin, *Crit. Rev. Toxicol.*, 2005, **35**, 379–411.
14 W. G. Kreyling, M. Semmler-Behnke, S. Takenaka and W. Möller, *Acc. Chem. Res.*, 2013, **46**, 714–722.
15 H. S. Choi, Y. Ashitate, J. H. Lee, S. H. Kim, A. Matsui, N. Insin, M. G. Bawendi, M. Semmler-Behnke, J. V. Fangioni and A. Tsuda, *Nat. Biotechnol.*, 2010, **28**, 1300–1303.
16 A. Buckley, J. Warren, A. Hodgson, T. Marczylo, K. Ignatyev, C. Guo and R. Smith, *Part. Fibre Toxicol.*, 2017, **14**, 5.
17 H. E. Shim, S. Mushtaq, L. Song, C. H. Lee, H. Lee and J. Jeon, *Bioorg. Med. Chem. Lett.*, 2018, **28**, 2875–2878.
18 L. Cavina, D. van der Born, P. H. M. Klaren, M. C. Feiters, O. C. Boerman and F. P. J. T. Rutjes, *Eur. J. Org. Chem.*, 2017, 3387–3414.
19 H. E. Shim, J. Y. Lee, C. H. Lee, S. Mushtaq, H. Y. Song, L. Song, S.-J. Choi, K. Lee and J. Jeon, *Chemosphere*, 2018, **207**, 649–654.
20 J. L. Burkemper, T. A. Aweda, A. J. Rosenberg, D. M. Lunderberg, G. F. Peaslee and S. E. Lapi, *Environ. Sci. Technol. Lett.*, 2017, **4**, 211–215.
21 L. Mao, M. Hu, B. Pan, Y. Xie and E. J. Petersen, *Part. Fibre Toxicol.*, 2016, **13**, 7.
22 B. Li, J. Yang, Q. Huang, Y. Zhang, C. Peng, Y. Zhang, Y. He, J. Shi, W. Li, J. Hu and C. Fan, *NPG Asia Mater.*, 2013, **5**, e44.
23 S. J. Lupton, J. K. Huwe, D. J. Smith, K. L. Dearfield and J. J. Johnston, *J. Agric. Food Chem.*, 2012, **60**, 1128–1134.
24 F. Marquet, J.-P. Payan, D. Beydon, L. Wathier, M.-C. Grandclaude and E. Ferrari, *Arch. Toxicol.*, 2011, **85**, 1035–1043.
25 D. A. Jasim, C. Ménard-Moyon, D. Bégin, A. Bianco and K. Kostarelos, *Chem. Sci.*, 2015, **6**, 3952–3964.
26 V. Georgakilas, J. N. Tiwari, K. C. Kemp, J. A. Perman, A. B. Bourlinos, K. S. Kim and R. Zboril, *Chem. Rev.*, 2016, **116**, 5464–5519.
27 X. Ji, L. Ciu, Y. Xu and J. Liu, *Compos. Sci. Technol.*, 2015, **106**, 25–31.

